



CERN-ACC-NOTE-2023-0006

2023-0006

Themistoklis.Mastoridis@cern.ch

HL-LHC Crab Cavity Field Regulation and Resulting RF Noise Spectrum

P. Baudrenghien

SY-RF, CERN

T. Mastoridis

California Polytechnic State University, San Luis Obispo, USA

Keywords: LHC, HL-LHC, RF, noise spectrum, crab cavities

Abstract

The HL-LHC Low Level RF (LLRF) must fulfill three requirements: it must reduce the cavity impedance at the fundamental below the instability threshold, it must regulate the crab cavity voltage precisely (amplitude and phase), and it must provide a cavity field with a spectral purity resulting in negligible degradation of the integrated luminosity due to transverse emittance growth. In this note, we present a LLRF system that fulfills these objectives. We then provide an estimate of the crab cavity RF noise spectrum for this LLRF system, a key parameter to evaluate transverse emittance growth.

Contents

1	HL-LHC Crab Cavity Low-Level RF	1
2	One-Turn Feedback	2
3	Transverse Emittance Growth due to Crab Cavity RF Noise	3
4	HL-LHC Crab Cavity RF Noise Spectrum Estimate	5
5	Crab Cavity RF Noise during the Cycle	7
6	Conclusions	9
7	Acknowledgments	9
	References	9

1 HL-LHC Crab Cavity Low-Level RF

The HiLumi LHC crab cavity will be driven by a tetrode or an inductive output tube (IOT) and regulated by the LLRF system. A simplified diagram of the crab cavity RF is shown in Figure 1.

The LLRF system will include a tuning loop to keep the cavity resonant frequency on-tune with the beam during the crabbing operation. For a crab cavity, the beam loading (if the beam is off-center) is aligned with the cavity voltage. Therefore, the optimal is to keep the cavity on tune, independently of the beam current.

The LLRF also includes a polar loop. This is a slow regulation loop around the amplifier to compensate for amplifier gains and phase drift, and to reduce the amplifier noise in a band extending to a few tens of kHz.

The RF feedback will control the cavity field to reduce the cavity impedance at the fundamental and for precise manipulations of crab cavity voltage and phase. It will consist of both a fast local loop around the cavity-amplifier and a slower global loop regulating the vector sum of voltages on the two sides of the interaction point (IP) [1]. The 400 MHz antenna signal is demodulated by the RF clock to baseband. The output of the polar loop is modulated back to 400 MHz.

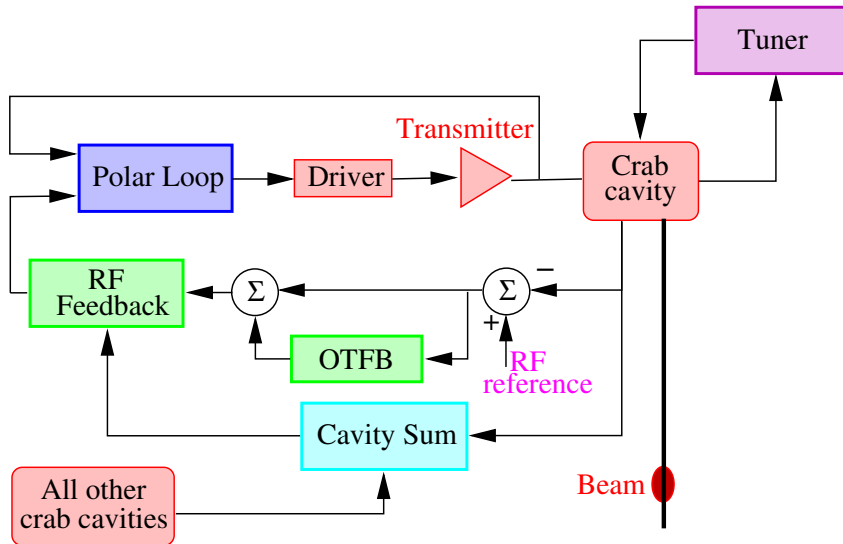


Figure 1: Crab Cavity Low-Level RF block diagram.

Good field control is essential not only for longitudinal impedance reduction and beam loading compensation, but also for the following reasons. During filling/ramping precise cavity counter-phasing is necessary to null the crabbing. When the HiLumi LHC is coasting at high energy and protons are colliding, the total kick from all crab cavities should lead to zero crabbing outside the interaction region. A strong regulation is also required to compensate for the beam loading if the beam is not centered.

The loop delay for each individual system will be about $1.3 \mu s$, including the transmitter delay (at most 100 ns). The delay limits the gain of a proportional RF feedback to 151 (linear) to achieve a 10 dB gain margin for a cavity Q_L of 500,000 and R/Q of 215Ω , resulting in a closed-loop bandwidth of 136 kHz. Figure 2 shows the Crab Cavity impedance without RF feedback (Open Loop) and with RF Feedback (Closed Loop). The fundamental impedance at the RF frequency is reduced by a factor of about 150.

If a global controller between cross-IP cavities is used, the delay will be about $3 \mu s$. The slower global feedback will result in zero crabbing outside the interaction region. In the case

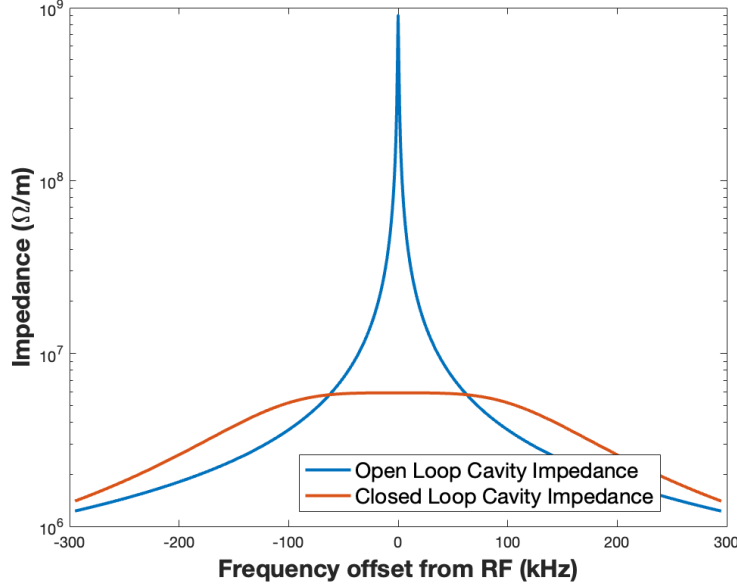


Figure 2: HiLumi LHC Crab Cavity impedance.

of a rapid change of the field in one cavity (for example a fast quench or a transmitter trip), the LHC Beam dump System will act to extract the beam in a maximum time of three turns ($267 \mu\text{s}$). The global controller should minimize the effect on the beam within the three turns to avoid abrupt displacements which can potentially damage the collimators.

2 One-Turn Feedback

The reduction of the crab cavity impedance by the RF feedback will *not* be sufficient to achieve stability [2]. A One-Turn Feedback (OTFB) system will be required for further impedance control [3]. Such systems are widely used to compensate for the transient beam loading in accelerating cavities. In that case the impedance is reduced on the revolution frequency sidebands (or the synchrotron sidebands around each revolution harmonic) [4], [5], [6]. The OTFB system will supplement the RF Feedback as shown in Figure 1, by acting at the betatron sidebands of the revolution harmonics to further reduce the impedance (H_{OTFB} in Figure 3). The width of the peaks at the betatron sidebands should be higher than the tune spread. A tradeoff exists between the peak width and OTFB gain, which is currently set to 10. The OTFB path will also include a low-pass filter, with a bandwidth close to the closed-loop cavity bandwidth. Finally, the OTFB path includes a delay $T_{rev} - \tau_c$ to make the total OTFB delay *almost* equal to the revolution period. The slight offset (τ_c) maximizes the loop stability by increasing the phase margins at the non-linear part of the phase response [4].

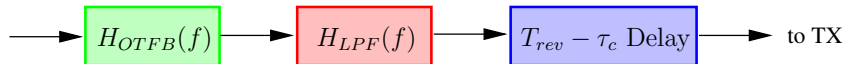


Figure 3: OTFB Block Diagram.

The OTFB response is given by

$$H_{OTFB}(\Delta\omega) = G_c \left[\frac{(1 - \alpha_c)e^{i2\pi\nu_b}}{1 - \alpha_c e^{i2\pi\nu_b} e^{-iT_{rev}\Delta\omega}} + \frac{(1 - \alpha_c)e^{-i2\pi\nu_b}}{1 - \alpha_c e^{-i2\pi\nu_b} e^{-iT_{rev}\Delta\omega}} \right]$$

where G_c is the OTFB gain, the parameter α_c controls the filter bandwidth around each betatron sideband, ν_b is the betatron tune, T_{rev} is the revolution period, $\Delta\omega$ is the angular frequency offset from the crab cavity resonance, and τ_c is the OTFB delay offset.

Figure 4 shows the Crab Cavity impedance with and without the OTFB (RF Feedback on for both traces). The impedance is reduced by a factor of ≈ 10 at all the betatron sidebands within the RF feedback closed-loop bandwidth. Figure 5 shows the impedance with the OTFB

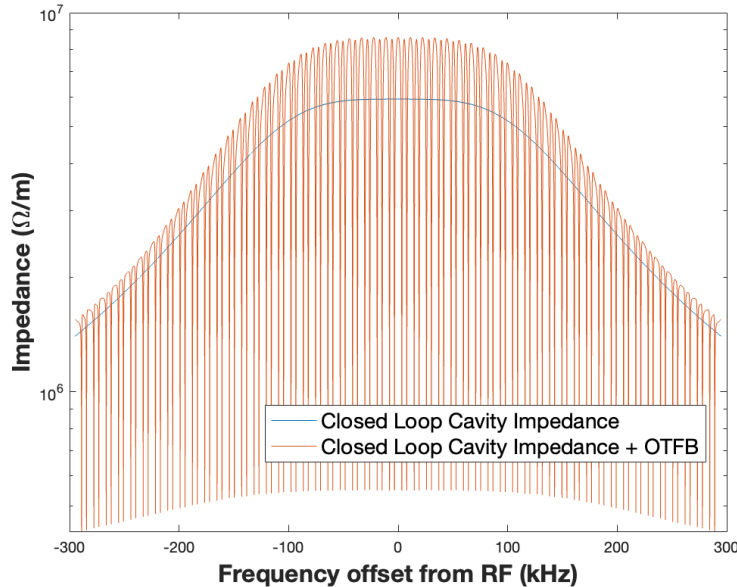


Figure 4: HiLumi LHC Crab Cavity impedance with OTFB.

over a span of one revolution frequency ($G_c = 10$, $\nu_b = 0.3$, $\alpha_c = 31/32$). The impedance is reduced at the two betatron sidebands.

3 Transverse Emittance Growth due to Crab Cavity RF Noise

The emittance growth rate due to phase and amplitude noise were derived by the authors in [7].

$$\frac{d\epsilon_n}{dt} = \gamma\beta_{cc} \left(\frac{eV_o f_{rev}}{2E_b} \right)^2 C_{\Delta\phi}(\sigma_\phi) \sum_{k=-\infty}^{\infty} S_{\Delta\phi} [(k \pm \bar{\nu}_b) f_{rev}] \quad (1)$$

$$C_{\Delta\phi}(\sigma_\phi) = e^{-\sigma_\phi^2} \left[I_0(\sigma_\phi^2) + 2 \sum_{l=1}^{\infty} I_{2l}(\sigma_\phi^2) \right]$$

$$\frac{d\epsilon_n}{dt} = \gamma\beta_{cc} \left(\frac{eV_o f_{rev}}{2E_b} \right)^2 C_{\Delta A}(\sigma_\phi) \sum_{k=-\infty}^{\infty} S_{\Delta A} [(k \pm \bar{\nu}_b \pm \bar{\nu}_s) f_{rev}] \quad (2)$$

$$C_{\Delta A}(\sigma_\phi) = e^{-\sigma_\phi^2} \sum_{l=0}^{\infty} I_{2l+1}(\sigma_\phi^2)$$

where ϵ_n is the normalized horizontal transverse emittance (assuming a horizontal crabbing scheme. Equations hold for vertical emittance in case of vertical crabbing), β_{cc} is the beta function at the crab cavity location (in m), e is the charge of a proton, V_o is the voltage of the crab cavity, f_{rev} is the revolution frequency, E_b the beam energy, σ_ϕ the rms bunch length (in

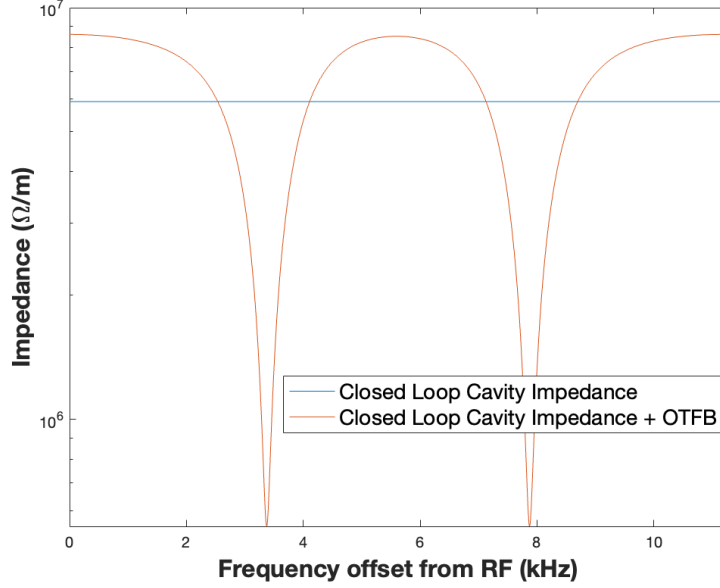


Figure 5: HiLumi LHC Crab Cavity impedance with OTFB.

radians with respect to the RF frequency), I is the modified Bessel function of the first kind, $\bar{\nu}_b$ is the non-integer betatron tune averaged over the particles, $\bar{\nu}_s$ is the mean synchrotron tune, and $S_{\Delta\phi}$, $S_{\Delta A}$ are the phase and (relative) amplitude noise power spectral density respectively (with units of rad^2/Hz and $1/\text{Hz}$ respectively). The voltage power spectral density is $S_{\Delta V} = V_o^2 S_{\Delta A}$. The \pm sign refers to upper and lower sidebands. As the crab cavity RF has zero phase at the center of the bunch, phase noise kicks lead to a shift of the bunch's centroid position, whereas amplitude noise leads to a rotation of the bunch around its centroid. The factors $C_{\Delta\phi}(\sigma_\phi)$ and $C_{\Delta A}(\sigma_\phi)$ correspond to normal distributed bunches and express the effect of bunch length on the transverse emittance growth [7].

From Equations 1, 2 it is clear that the emittance growth depends on accelerator parameters, the bunch length ($C_{\Delta\phi}(\sigma_\phi)$ and $C_{\Delta A}(\sigma_\phi)$), and the noise power spectral density sampled at the betatron or synchro-betatron sidebands of all revolution harmonics. The emittance growth rate depends on the bunch length because the HiLumi LHC bunch length (1 ns 4σ) is a significant portion of the RF period (2.5 ns), so the momentum kicks from the crab cavities are not simply proportional to the z position of the particles.

For phase noise (Equation 1), the “effective” noise power is the sum of the phase noise Power Spectral Density (PSD) sampled on all betatron sidebands (two per revolution frequency line). For amplitude noise (Equation 2) we must sum the amplitude noise PSD on all synchro-betatron sidebands (four per revolution frequency line). This suggests the introduction of an effective PSD defined as:

$$\sum_{k=-\infty}^{\infty} S_{\Delta\phi} [(k \pm \bar{\nu}_b) f_{rev}] = 2S_{\Delta\phi,\text{eff}}(\bar{\nu}_b f_{rev})$$

$$\sum_{k=-\infty}^{\infty} S_{\Delta A} [(k \pm \bar{\nu}_b \pm \bar{\nu}_s) f_{rev}] = 4S_{\Delta A,\text{eff}}(\bar{\nu}_b f_{rev})$$

$S_{\Delta\phi,\text{eff}}(f)$, $S_{\Delta A,\text{eff}}(f)$ are the *aliased* power spectral densities extending from $-f_{rev}/2$ to $f_{rev}/2$ that lead to the same total noise power sampled by the beam.

The phase noise emittance growth rate is reduced by the LHC transverse damper by a

correction factor of \bar{R}_d [7].

$$\begin{aligned}\bar{R}_d &= \frac{1}{\pi} \int_{-\infty}^{\infty} g(u) \left\{ 1 - \frac{e^{-\sigma_\phi^2}}{C_{\Delta\phi}(\sigma_\phi)} \frac{\alpha^2(g(u)^2 + f(u)^2) + 2\alpha g(u)}{(1 + \alpha g(u))^2 + (\alpha f(u))^2} \right\} du \\ \alpha &= \frac{G}{4\pi\sigma_{\nu_b}}\end{aligned}\tag{3}$$

where G is the LHC transverse damper gain, σ_{ν_b} is the rms betatron tune spread, and $f(u)$, $g(u)$ are scaled versions of the real and imaginary parts of the beam transfer function [7]. In this work we use a distribution dominated by head-on beam-beam effects, with smaller, but not insignificant chromaticity contributions, as shown in Figure 12 in [7]. The correction factor has some dependence on the assumed tune distribution (up to 20%), as shown in Figure 8 in [7].

The LHC transverse damper has sufficient bandwidth to generate independent kicks for each bunch (25 ns spacing) but the kick is constant over the bunch. It is therefore not efficient in compensating phase noise kicks, as they generate a co-sinusoidal kick along the bunch [7]. In addition, the damper cannot act on amplitude noise because the mean bunch position is not changed due to amplitude noise. For the HL-LHC operational parameters, the transverse damper will reduce phase noise effects by a factor $\bar{R}_d = 0.32$ for $G = 0.04$ (corresponds to 50 turns damping time in physics [8]).

4 HL-LHC Crab Cavity RF Noise Spectrum Estimate

An estimate of the crab cavity RF noise power spectrums $S_{\Delta\phi}(f)$ and $S_{\Delta A}(f)$ is necessary to evaluate the RF noise sampled by the beam. This section presents the RF noise spectrum measured in the LHC accelerating cavities (ACS) and the expected improvements for the crab cavity system. Even though the emittance growth only depends on the aliased power spectral density, analyzing the complete spectrum is informative on the components that increase the noise spectrum the most.

The single-sideband phase noise power spectral density $L(f)$ measured at the **main RF system** in the LHC (accelerating 400 MHz cavities) is shown in Figure 6, reported in units of dBc/Hz, where dBc stands for “dB below carrier”. The RF Reference is the output of the Voltage-Controlled Crystal Oscillator (VCXO) generating the reference for all eight cavities of a given ring. The Main RF cavity signal is a measurement of the antenna signal of one cavity. $L(f)$ is the most common measurement of RF phase noise. $S(f)$ is the phase noise power spectral density in rad^2/Hz , and it is given by $S(f) = 10^{L(f)/10}$ [9], $S(-f) = S(f)$, for $f \geq 0$ ¹. The asterisks in the figure correspond to the first forty betatron sidebands, frequencies that contribute to total noise power sampled by the beam (Equations 1, 2). The LHC revolution frequency is 11.245 kHz. The non-integer horizontal betatron tune is 0.31. This spectrum can be separated in four bands of interest:

- $1/f^3$ noise in the 0-5 Hz range, which is of no consequence for emittance growth as it is lower than the first betatron sideband (≈ 3 kHz).
- RF reference noise in the 10 Hz to 1 kHz range (also below the first betatron sideband for the LHC main RF system) which only contributes to crab cavity phase noise.
- Transmitter noise is important in the band extending to ≈ 20 kHz. It is reduced by the RF Feedback and Polar loops. 70% of the estimated noise is due to the two sidebands at this band!

¹We define $S(f)$ as the Fourier Transform of the noise autocorrelation function. The IEEE standard defines $S(f)$ for positive frequencies only and has thus twice the value of our definition, which is valid for all frequencies.

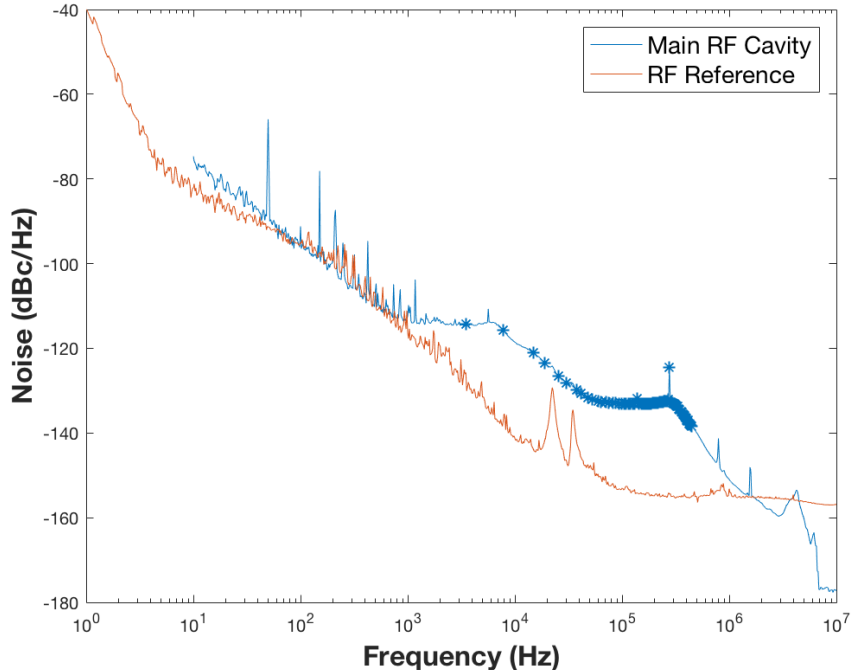


Figure 6: LHC accelerating cavity (ACS), and RF Reference phase noise.

- In the presence of the very strong RF feedback, the noise level in the 20-400 kHz range is defined by the demodulation of the cavity antenna signal (receiver noise). It extends to the end of the feedback bandwidth (350 kHz for the ACS system).

For the crab cavity case, the RF reference will be much cleaner. The LHC Accelerating Cavity LLRF uses RF synchronous clocks and a VCXO generated analog RF reference for demodulation/modulation. The Crab Cavity LLRF will use the architecture introduced for the SPS LLRF upgrade [10], [11]: Fixed frequency clocks – including the demodulator/modulator Local Oscillator (LO) –, transmission of the RF frequency as numerical word via the White Rabbit link, and synchronous demodulation via Numerically Controlled Oscillator (NCO). Fixed frequency clocks and LO can easily be cleaned using narrowband Phase-Locked Loops. Tetrodes and IOTs are less noisy than klystrons (used in the accelerating system), so the noise level in the third band will be reduced below the demodulator noise level after the action of the crab cavity feedback loops. Finally, in the fourth band, an improved demodulator will bring the noise level down to about -143 dBc/Hz (this is comparable to the lowest noise levels achieved at other accelerators since the LHC commissioning [12], [13]). This is a *significant* reduction by ≈ 10 dB from the LHC accelerating system levels.

The resulting estimate for the crab cavity phase noise is shown in Figure 7. The noise in the RF reference (clocks and LO) is assumed to drop below -143 dBc/Hz by the first betatron line. The noise spectrum drops after 136 kHz due to the reduced feedback bandwidth as mentioned in Section 1.

The transmitter noise will be significantly reduced by the polar loop (by at least 40 dB). As a result, the crab cavity amplitude noise will be dominated by the demodulator noise and the bandwidth of the RF feedback. The feedback will be implemented in I/Q coordinates after demodulation to baseband. The demodulator phase and amplitude noise spectra will be identical in the absence of LO noise or at high enough frequencies where the LO/RF reference noise is low, which is the case at the HL-LHC betatron sidebands.

Using the above phase noise spectrum, and assuming identical $S_{\Delta\phi}(f)$ and $S_{\Delta A}(f)$ spectra,

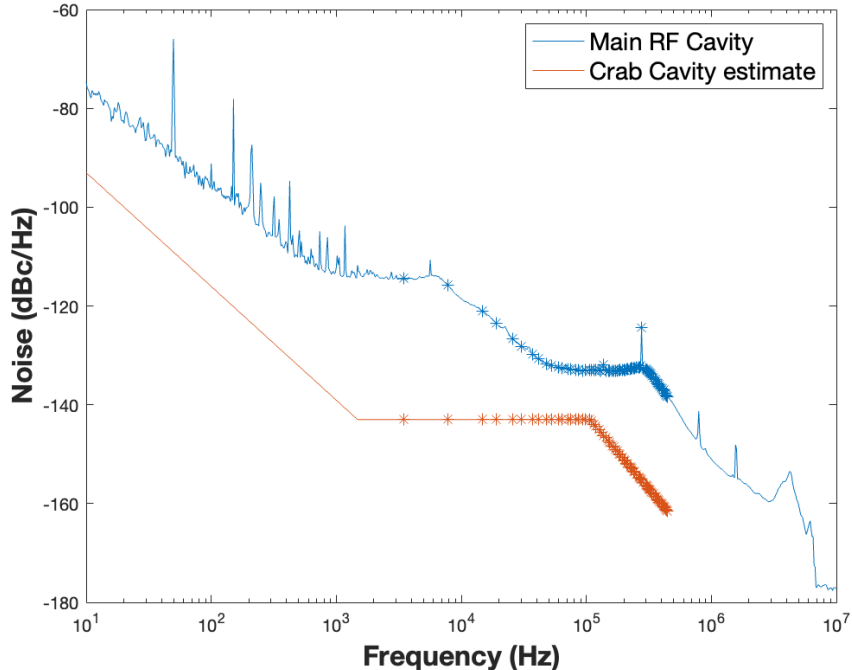


Figure 7: LHC accelerating cavity (measured) and crab cavity (estimated) phase noise.

we use Equations 1, 2 to calculate the growth rate with the parameters during physics (7 TeV, 3.4 MV/cavity, four cavities per beam and per plane with uncorrelated noise, and $\beta_{cc} = 3620$ m). The effect of the transverse damper is included in the emittance growth calculation (phase noise) assuming a damping time of fifty turns. The resulting emittance growth rate will be 7.6%/hour and 9.0%/hour due to phase and amplitude noise respectively, leading to a total emittance growth of about 16.6%/hour. The emittance growth rate in this realistic scenario is significantly higher than the HL-LHC target (2%/hour in physics with $\beta^*=0.15$ m) [8]. Therefore, additional mitigation is required to reach and exceed the luminosity lifetime goals. A dedicated Crab Cavity RF noise feedback system is proposed to reduce the effects of RF noise and thus relax the RF noise thresholds [14].

5 Crab Cavity RF Noise during the Cycle

Equations 1, 2 show the emittance growth dependance on accelerator parameters. Crabbing at $380 \mu\text{rad}$ full angle will be applied from the beginning of physics. The HL-LHC is intended to operate the crab cavities with a fixed 3.4 MV (per cavity) during collision. It will also employ β^* leveling: β^* will be reduced from 0.64 to 0.15 m during Physics, which in turn leads to an increase of β_{CC} for a constant full crabbing angle and voltage. As a result, the transverse emittance growth rate due to crab cavity noise will increase during the fill, and will be maximized at the end of the physics fill (minimum β^*).

The actual β^* leveling procedure might be adjusted before HL-LHC starts operating. Options considered include starting collisions with β^* larger than 0.64 m, or terminating collision with a β^* of 0.18 m. In all cases the final value at the end of the cycle will be 0.15 m or more. In this work we use 0.15 m, which leads to the most challenging transverse emittance growth rate, and is thus a conservative estimate.

Before the start of Physics, crabbing is not needed nor desired, and thus there is an option to keep the crab cavities off. This is not ideal, because then there is no control of the cavity

tune, which could intersect a betatron line during the acceleration ramp leading to transverse instabilities. The HL-LHC crab cavities have sufficient tuning range to follow the acceleration ramp. So, alternatively, the crab cavities can be kept on at a reduced voltage (300 kV) during filling and ramping, with counter-phasing on, so that the total crabbing voltage is zero, while maintaining active control of cavity tune and field. This is the current operational scenario.

As shown in Section 4, the RF noise is dominated by the RF demodulator. As such, and depending on the final RF/LLRF architecture, it is possible that the RF noise levels will be independent of the voltage. Two noise scenarios are thus investigated:

- Realistic: The Crab Cavities are at 300 kV until right before Physics and the noise effects scale with the voltage.
- Worst case: The noise level is independent of the voltage. This is equivalent to the Crab Cavities being at 3.4 MV throughout the cycle.

The noise scaling term due to accelerator parameters from Equations 1, 2 is

$$C_{AP} = N_{cc} \gamma \beta_{cc} \left(\frac{eV_o f_{rev}}{2E_b} \right)^2$$

where N_{cc} is the number of cavities per beam and per plane ($N_{cc} = 4$) and we are assuming uncorrelated noise. Figure 8 shows C_{AP} during the cycle for the two noise scenarios. The noise scaling term is maximum at the end of physics (lowest β^*). The integrated contributions are

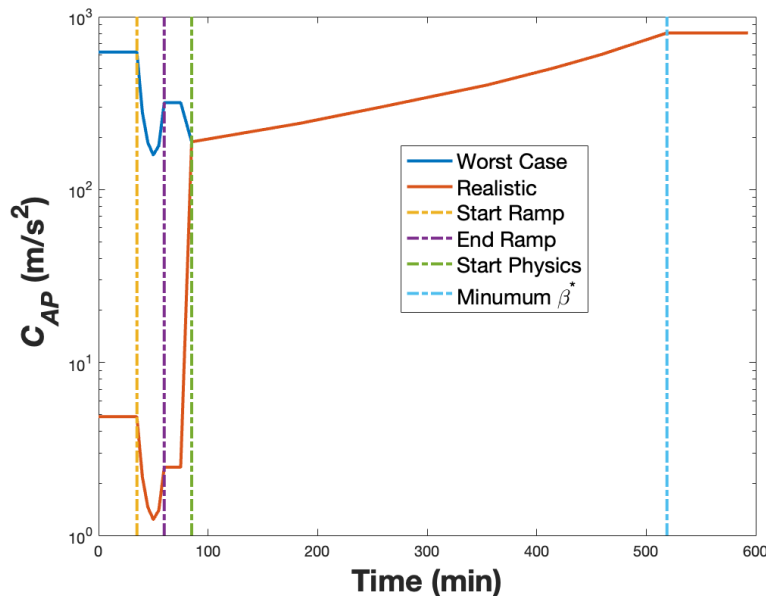


Figure 8: Operational parameters scaling during the cycle. β^* leveling from Start of Physics until the minimum value is reached.

1.47e7 and 1.250e7 m/s for the worst and realistic cases respectively. The worst case is about 18% higher.

The RF front-end gain could be adjusted during the fill to always cover the full ADC range. As a result, the digitization noise early in the fill will be much lower (as transformed into volts) and we will effectively return to the realistic case scenario.

The HiLumi LHC has a target of 1% integrated luminosity loss due to crab cavity induced transverse emittance growth [15]. The *integrated* emittance growth due to RF noise was estimated as a function of the crabbing voltage and β^* during the HL-LHC cycle for the realistic scenario, resulting in a 2%/hour emittance growth threshold at the end of the physics fill [8].

6 Conclusions

This Note outlines the planned Field Regulation in the HL-LHC Crab Cavity and derives the expected RF noise spectrum. It identifies the major noise sources and summarizes the necessary improvements to achieve a *reasonable* emittance growth rate. Even with these significant improvements, the noise threshold will be exceeded, requiring further mitigation, such as the proposed Crab Cavity RF noise feedback system [14], [16].

7 Acknowledgments

We thank E. Metral, R. Tomas, N. Mounet, X. Buffat, L. Giacometti (CERN) for their explanations on the HL-LHC physics parameters and on the possible crab cavity impact on stability. The HL-LHC crab cavity RF project is led by R. Calaga. We thank him for the support in developing a LLRF for this future system and for the effort investigating emittance growth with the SPS crab cavity test stand.

Research supported by the HL-LHC project. This work is supported by the U.S. Department of Energy, Office of Science, Office of High Energy Physics, under Award Number DE-SC-0019287.

References

- [1] “High-Luminosity Large Hadron Collider: Technical Design Report”, CERN-2017-007-M, 2017.
- [2] L. Giacometti, X. Buffat, N. Mounet, “Update from the impedance and instabilities studies”, <https://indico.cern.ch/event/1237188/>.
- [3] L. Giacometti, X. Buffat, N. Mounet, R. Calaga, P. Baudrenghien, “Effectiveness of the Betatron Comb filter for Mitigating the CCs Fundamental Mode Impedance”, <https://indico.cern.ch/event/1253310/>.
- [4] T. Mastoridis, P. Baudrenghien, J. Molendijk, “The LHC One-Turn Feedback”, ATS-Note-2012-025 PERF, February 2012.
- [5] P. Baudrenghien, G. Lambert, “Reducing the impedance of the travelling wave cavities: feed-forward and one turn delay feed-back”, 10th Workshop on LEP-SPS Performance, Chamonix, France, 17 - 21 Jan 2000, pp. 94-101.
- [6] F. Pedersen, “RF Cavity Feedback”, CERN-PS-92-59-RF, December 1992.
- [7] P. Baudrenghien, T. Mastoridis, “Transverse emittance growth due to rf noise in the high-luminosity LHC crab cavities”, Phys. Rev. ST Accel. Beams 18, 101001 (2015).
- [8] E. Metral *et. al.*, “Update of the HL-LHC Operational Scenarios for Proton Operation”, CERN-ACC-NOTE-2018-0002, January 2019.
- [9] “IEEE Standard Definitions of Physical Quantities for Fundamental Frequency and Time Metrology-Random Instabilities”, in IEEE Std 1139-1999 , pp.1-40, 21 July 1999.
- [10] A. Spierer, P. Baudrenghien, J. Egli, G. Hagemann, P. Kuzmanovic, I. Stachon, M. Suminski, T. Wlostowski, “The CERN SPS Low Level RF: The Beam-Control”, 13th International Particle Accelerator Conference (IPAC 2022), Bangkok, Thailand, 12 - 17 Jun 2022.

- [11] G. Hagmann, P. Baudrenghien, J. Egli, A. Spierer, M. Suminski, T. Wlostowski, “The CERN SPS Low Level RF: The Cavity-Controller”, 13th International Particle Accelerator Conference (IPAC 2022), Bangkok, Thailand, 12 - 17 Jun 2022.
- [12] G. Huang, L. Doolittle, J. Yang, Y. Xu, “Low Noise Digitizer Design for LCLS-II LLRF”, Proceedings of NAPAC 2016, Chicago, IL.
- [13] G. Huang *et. al.*, “High Precision RF Control for the LCLS-II”, Proceedings of NAPAC 2016, Chicago, IL.
- [14] P. Baudrenghien, T. Mastoridis, “Transverse Emittance Growth due to RF Noise in Crab Cavities: Theory, Measurements, Cure, and High Luminosity LHC estimates”, prepared for publication.
- [15] G. Arduini *et. al.*, “HL-LHC Run 4 proton operational scenario”, CERN-ACC-2022-0001, June 2022.
- [16] P. Baudrenghien, T. Mastoridis, B. Miller, “Crab Cavity RF Noise Feedback and Transverse Damper Interaction”, CERN-ACC-NOTE-2019-0006, February 2019.